

# Microwave Photonic Interrogation of a High-Speed and High-Resolution Multipoint Refractive Index Sensor

Guangying Wang<sup>1</sup>, Baoliang Liao, Yuan Cao<sup>1</sup>, Tuan Guo<sup>1</sup>, *Senior Member, IEEE*, Xinhuan Feng<sup>1</sup>, Bai-Ou Guan<sup>2</sup>, *Member, IEEE*, and Jianping Yao<sup>2</sup>, *Fellow, IEEE*

**Abstract**—Microwave photonic interrogation of a high-speed and high-resolution multipoint refractive index (RI) sensor based on an Au-coated tilted fiber grating (Au-TFBG) array is proposed and experimentally demonstrated. Due to the surface plasmon resonance (SPR), the optical spectrum of an Au-TFBG has a dip in the spectral envelope. When an Au-TFBG is immersed in a solution and the RI of the solution changes, the location of the dip will shift, reflecting the change of the RI. For multipoint sensing, an Au-TFBG array with the array elements located at different locations is employed. However, due to the overlap of the spectra of the Au-TFBGs in the array, the dips cannot be precisely located by optical spectrum measurement. A solution is to convert the spectra to the time domain based on spectral shaping and wavelength-to-time (SS-WTT) mapping with the mapped temporal waveforms separated by different time delays. By using a digital signal processor (DSP), the sensing information can be extracted at a high speed and high resolution. The proposed approach is evaluated experimentally. Experimental results show that the sensor has high RI accuracies of  $3.1 \times 10^{-5}$ ,  $2.5 \times 10^{-5}$  and  $2.6 \times 10^{-5}$  refractive index unit (RIU) and a fast sensing speed of 11.75 kHz.

**Index Terms**—Envelope detection, microwave photonics, multipoint refractive index measurement, surface plasmonic resonance, tilted fiber Bragg grating array.

## I. INTRODUCTION

MEASUREMENTS of refractive index (RI) based on optical fiber sensors could find enormous applications such as biomedical detections [1], [2] and chemical analysis [3] due to

Manuscript received March 23, 2021; revised August 17, 2021; accepted November 6, 2021. Date of publication November 15, 2021; date of current version February 16, 2022. This work was supported in part by National Natural Science Foundation of China under Grants 61860206002, 61701193, 61771221, 62035006 and 61975068, in part by the Natural Science Foundation of Guangdong Province General Program under Grant 2021A1515011944, and in part by the Local Innovative and Research Teams Project of Guangdong Pearl River Talents Program under Grant 2019BT02X105. (*Corresponding authors: Yuan Cao; Xinhuan Feng.*)

Guangying Wang, Baoliang Liao, Yuan Cao, Tuan Guo, Xinhuan Feng, and Bai-Ou Guan are with the Guangdong Province Key Laboratory of Optical Fiber Sensing and Communications, Institute of Photonics Technology, Jinan University, Guangzhou 510632, China (e-mail: guangyingwang@stu2017.jnu.edu.cn; baoliang@stu2019.jnu.edu.cn; caoyuan@jnu.edu.cn; tuanguo@jnu.edu.cn; eexhfeng@gmail.com; tguanbo@jnu.edu.cn).

Jianping Yao is with the Microwave Photonics Research Laboratory, School of Electrical Engineering and Computer Science, University of Ottawa, Ottawa, ON K1N 6N5, Canada (e-mail: jpyao@uottawa.ca).

Color versions of one or more figures in this article are available at <https://doi.org/10.1109/JLT.2021.3127239>.

Digital Object Identifier 10.1109/JLT.2021.3127239

their distinctive advantages such as compact size, remote sensing ability, high resistance to erosion, immunity to electromagnetic interference, and high tolerance to harsh environment [4]. In the recent years, several single point optical fiber RI sensors using a long period fiber grating (LPFG) [5], a tapered optical fiber [6], a tilted fiber Bragg grating (TFBG) [7]–[9], a photonic crystal fiber (PCF) [10], [11] and a D-shaped fiber [12] have been proposed and experimentally demonstrated. For some applications such as real-time environment monitoring, food processing and packaging control, environment and contamination assessments, gas detection, and the structure health monitoring [4] where multiple points and quasi-distributed monitoring in a large range is highly demanded, a single point optical fiber sensor cannot meet the demand and a sensor that can provide a multipoint or quasi-distributed monitoring ability is highly required. To achieve multipoint or quasi-distributed sensing, a series of sensors are placed at different locations to monitor the change of sensing information. Recently, a quasi-distributed RI sensor based on cascaded microfiber Fabry-Perot interferometers using wavelength division multiplexing (WDM) method has been reported [13]. For WDM technique, the most outstanding advantage is its simplicity. However, to prevent crosstalk between different sensor elements, the operating bandwidth of each sensor element should be narrow to avoid spectrum overlap. Thus, for a given overall bandwidth, the number of the sensor elements is limited. Moreover, using an optical spectrum analyzer (OSA) to scan the whole spectral range of the sensor array, the sensing system always has a low sensing accuracy and a slow sensing speed. On the other hand, a multipoint refractometer based on frequency division multiplexing (FDM) has been reported [14]. Although the multiplexing capacity is significantly improved, the complexity of the sensing system is increased since an unbalanced interferometer is used to generate a random intensity modulated reference signal. If the sensing information can be converted from the optical spectral domain to the time domain, the demodulation of the sensing information will become much easier and the complexity of the sensing system will be highly reduced.

Microwave photonics (MWP) [15], [16], a technique to generate and process microwave signals directly in the optical domain, has been widely studied which can find applications such as radars [17], communications [18] and modern instrumentation [19], [20]. On the other hand, MWP techniques can also be

employed to implement high-speed and high-resolution sensing, to translate the sensing information from the spectral domain to the time domain, which is particularly important for multipoint or quasi-distributed optical fiber sensing. Instead of measuring the spectra of a multipoint sensor array, the spectra of the sensor array are converted to the time domain based on spectral shaping and wavelength-to-time (SS-WTT) mapping [21]. By introducing different time delays between the sensor array elements, the spectral information, which may overlap in the spectral domain, are separated in the time domain. By using a digital signal processor (DSP) to process the time-domain signals, the sensing information can be demodulated.

In this paper, we propose and experimentally demonstrate a multipoint fiber-optic RI sensor based on an Au-TFBG array, which is interrogated based on an MWP technique, to translate the spectra of the array elements to the time domain. The sensor array consists of multiple distributed Au-TFBGs, in which the spectra of the array elements are overlapped, and the use of an optical spectral analyzer cannot demodulate the wavelength shifting information. Based on SS-WTT mapping, the spectra are mapped to the time domain. More importantly, the physical distance between adjacent sensor elements is also mapped to the time domain as a time delay difference, thus the mapped temporal waveforms are temporally separated, which makes it possible to interrogate the sensor elements even the spectra are overlapped in the frequency domain. A detailed discussion on the mapping of the physical distance between adjacent sensor elements to a time delay difference is performed. An experiment is then performed to evaluate the effectiveness of the proposed interrogation approach. Experimental results show that the proposed sensor can be effectively interrogated. For a sensor array consisting of three Au-TFBGs, the sensing accuracies are measured to be  $3.1 \times 10^{-5}$ ,  $2.5 \times 10^{-5}$  and  $2.6 \times 10^{-5}$  RIU refractive index unit (RIU), and the sensing speed is as high as 11.75 kHz.

## II. PRINCIPLE AND EXPERIMENTAL SETUP

The optical spectrum of an Au-TFBG has a comb like shape resulted from multiple cladding modes. If an Au-TFBG is immersed into a solution, due to the SPR effect, the Au-TFBG spectrum will have an envelope with a dip in the envelope. When the RI of the solution changes, the wavelength location of the dip in the envelope will shift, reflecting the change of the ambient RI. Due to the limited resolution of an OSA, the envelope cannot be accurately extracted and the wavelength location of the dip cannot be precisely measured in the optical domain. An effective solution is to convert the Au-TFBG spectrum to the time domain. Through envelop detection, the envelope with a dip is obtained, and the locations of the dips in the envelopes of the time domain waveforms indicate the sensing information of the Au-TFBG array.

The experimental setup of the proposed multipoint RI sensor is shown in Fig. 1(a). It consists of a Fourier domain mode-locked (FDML) laser source [22], an SOA, an Au-TFBG array consisting of three Au-TFBGs, a PD, a real-time oscilloscope, and a DSP. The FDML laser source is used to provide a high-speed and broadband frequency chirped optical pulse train. The SOA is used to block some of the optical pulses in the pulse train to reduce the repetition rate, as shown in Fig. 1(b). The repetition-rate-reduced pulse train is directed to the Au-TFBG sensor array. When the frequency chirped optical pulses are launched to the three Au-TFBGs, the spectra of the pulses are spectrally shaped and the sensing information is encoded. To separate the three spectrally shaped optical pulses in the time domain, three optical delay lines with different lengths are inserted into the sensor array. A PD is then used to detect the spectrally shaped optical pulses where wavelength-to-time mapping is implemented, and three temporal microwave waveforms are generated. A real-time oscilloscope is employed to sample the time domain signals and a DSP is used to demodulate the sensing information at high speed and high resolution.

One important device in the sensing system is the FDML laser source. It is a fiber ring laser with a tunable optical filter (TOF) incorporated in the ring cavity to achieve Fourier-domain mode locking. Since the TOF is driven by a sinusoidal function, a chirped pulse with a positive chirp rate for the first half of the pulse and a negative chirp rate for the last part of the pulse, each having a time duration of  $T/2$  is generated. Mathematically, the relationship between the instantaneous wavelength and time of a pulse from a FDML laser source can be expressed by

$$\lambda(t) = \frac{\Delta\lambda}{2} \sin\left(2\pi ft - \frac{\pi}{2}\right) + \lambda_c \quad (1)$$

where  $\Delta\lambda$ ,  $f$ , and  $\lambda_c$  are, respectively, the wavelength scanning bandwidth, the repetition rate, and the central wavelength of a pulse generated by the FDML laser source.  $T = 1/f$  is the period of the pulse train.

The repetition rate of the generated pulse train is reduced by the SOA which is modulated by a periodic gate signal. The relationship between the instantaneous wavelength and time of the frequency-chirped optical pulse at the output of the SOA can be expressed by as in (2) shown at the bottom of the page, where  $M$  is an integer representing the repetition rate reduction factor.

Then, the repetition-rate-reduced pulse train is split into three paths and applied to the Au-TFBG sensor array, where the spectra in the three paths are shaped by the Au-TFBGs. Normally, the transmission spectrum of an Au-TFBG has a comb like shape resulted from cladding modes due to the tilted nature of the grating with a relatively flat intensity distribution. When the Au-TFBG is immersed into a solution, due to the SPR effect, a dip will be introduced to the envelope with the location of the dip reflecting the sensing information. Mathematically,

$$\lambda(t) = \begin{cases} \frac{\Delta\lambda}{2} \sin\left(2\pi ft - \frac{\pi}{2}\right) + \lambda_c, & nMT \leq t \leq nMT + \frac{T}{2} \\ \text{none}, & nMT + \frac{T}{2} < t < (n+1)MT \end{cases} \quad (2)$$

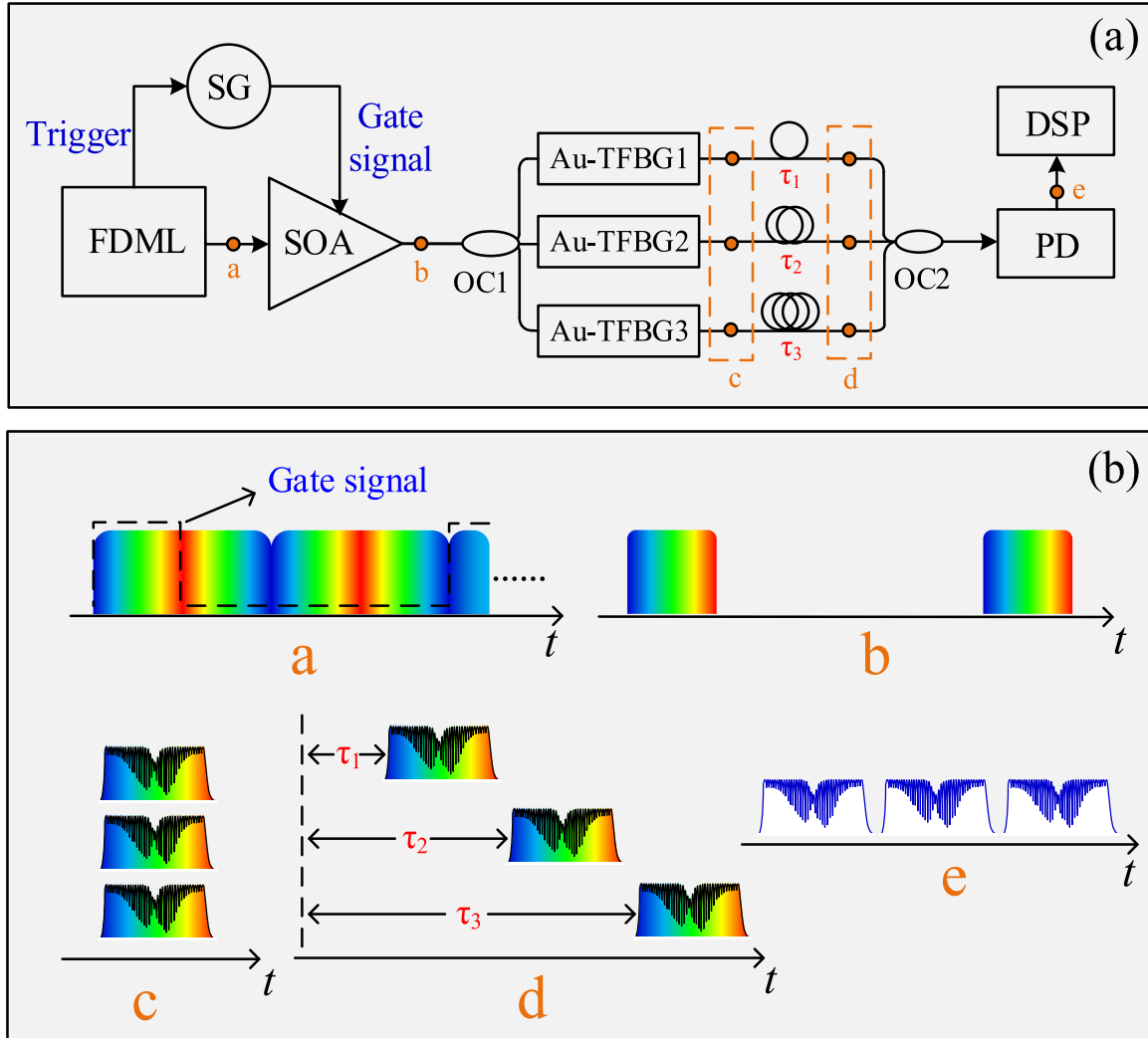


Fig. 1. (a) Experimental setup of the proposed multipoint RI sensor. (b) The waveforms at different locations of the sensor.

the transmission spectrum of an Au-TFBG sensor with SPR effect can be approximately expressed by

$$T(\lambda) \approx SPR(\lambda) \cdot \left[ \frac{1}{2} + \frac{1}{2} \cos\left(\frac{2\pi C}{\lambda}\right) \right] \quad (3)$$

where the first term is the SPR envelope and the second term describes the cladding mode distribution of the Au-TFBG spectrum with  $C$  a constant which is related to the wavelength spacing of the cladding modes.

The instantaneous output power of the frequency chirped optical pulse from the FDML laser can be considered constant, which is denoted as  $P_0$ . The instantaneous optical power at the output of the Au-TFBG can be given

$$P(t) = P_0 \cdot SPR[\lambda(t)] \cdot \left[ \frac{1}{2} + \frac{1}{2} \cos\left(\frac{2\pi C}{\lambda(t)}\right) \right] \quad (4)$$

Three fiber delay lines incorporated in the sensor array are used to separate the shaped pulses with different time delays. The spectrally shaped, and time-delayed optical pulses are then launched to a PD. Note that instead of using a dispersive element to achieve wavelength-to-time mapping, since the optical pulse

generated by the FDML laser source is frequency chirped, wavelength-to-time mapping is performed as the optical pulse is detected at the PD. After SS-WTT mapping, the optical spectra of the Au-TFBGs are mapped to the time domain and three temporal microwave waveforms separated by different time delays are generated at the output of the PD. The photocurrent can be expressed by

$$i_n(t) = \Re P_0 \cdot SPR_n[\lambda(t)] \cdot \left[ \frac{1}{2} + \frac{1}{2} \cos\left(\frac{2\pi C}{\lambda(t)}\right) \right] \quad (5)$$

where  $\Re$  denotes the responsivity of the PD, and  $n = 1, 2, 3$  stands for the waveforms resulted from Au-TFBG1, Au-TFBG2 and Au-TFBG3, respectively. A real-time oscilloscope is employed to sample the temporal microwave waveforms and an envelope detector consisting of a digital low-pass filter is used to extract the envelopes from the three time-domain signals with different time delays at a high-speed and high-resolution. The extracted envelopes can be expressed by

$$i'_n(t) = \frac{1}{2} \Re P_0 \cdot SPR_n[\lambda(t)] \quad (6)$$

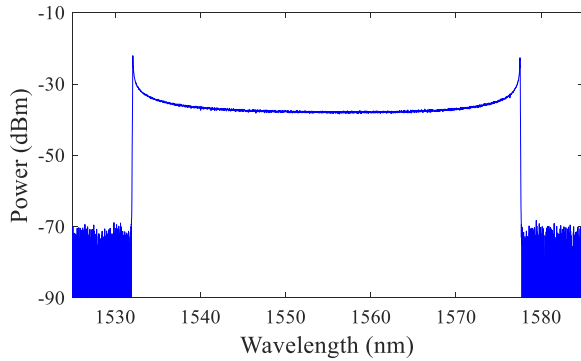


Fig. 2. The optical spectrum of the pulse generated by the FDML laser source. The center wavelength is 1555 nm and the bandwidth is 45 nm.

By monitoring the time shifts of the dips in the extracted envelopes, the sensing information is demodulated.

### III. EXPERIMENTAL RESULTS

An experiment based on the experimental setup shown in Fig. 1(a) is implemented. A broadband frequency chirped optical pulse train with a repetition rate of 23.5 kHz, a spectral bandwidth of 45 nm and a central wavelength of 1555 nm generated by an FDML laser source is applied to an SOA via an optical isolator. Fig. 2 shows the optical spectrum of the optical pulse generated by the FDML laser source. A gate signal with a repetition rate of 11.75 kHz (half of the repetition rate of the FDML laser source) and a duty cycle of 25 percent generated by a signal generator (SG) which is synchronized by the FDML laser source is used to modulate the SOA. Thus, the repetition rate of the optical pulse train is reduced by two times, which is 11.75 kHz.

The repetition-rate-reduced optical pulse train is split into three paths and applied to the Au-TFBG array. As the optical pulse is launched to an Au-TFBG, the spectrum is shaped and the sensing information is encoded. To separate the spectrally shaped pulses by different time delays, optical delay lines are implemented. In the first path, the shaped pulse is applied to the PD through a short pigtail with an approximately  $0 \mu\text{s}$  time delay. Meanwhile, a fiber delay line with a length of 4.5 km long is inserted into the second path to introduce a  $22.5 \mu\text{s}$  delay, and a second fiber delay line with a length of 9 km long is inserted into the third path to introduce a  $45 \mu\text{s}$  delay. At the output of the Au-TFBG array, the spectrally shaped optical pulses are combined and launched to a PD. Note that since the optical pulse of the FDML laser source is frequency chirped, wavelength-to-time (WTT) mapping is performed as the optical pulse is detected at the PD. By detecting the spectrally shaped optical pulses, three temporal microwave waveforms separated by two different time delays of  $22.5 \mu\text{s}$  and  $45 \mu\text{s}$  are generated.

Fig. 3 shows the temporal microwave waveforms generated at the output of a PD. As can be seen, through SS-WTT mapping, the optical spectra of the Au-TFBG sensor array are mapped to the time domain with different time delays and an SPR dip can be found in each of the three envelopes of the microwave waveforms.

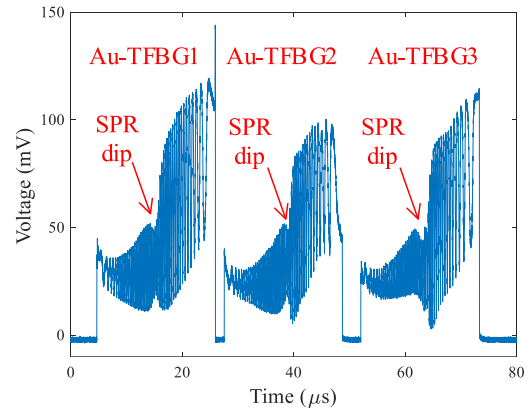


Fig. 3. Temporal microwave waveforms generated at the output of the PD.

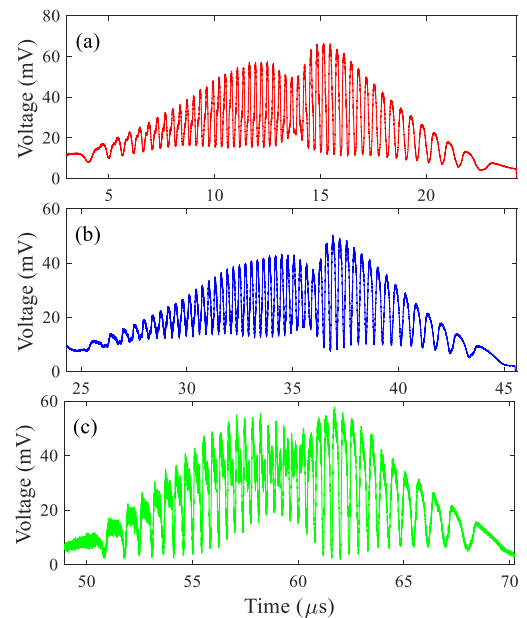


Fig. 4. The three temporal microwave waveforms resulted from (a) Au-TFBG1, (b) Au-TFBG2, and (c) Au-TFBG3, after shaped by a Gaussian window.

The microwave waveforms are sampled by a real-time oscilloscope and then sent to a DSP, to extract the location information of the dips. A Gaussian window is used to shape the sampled microwave waveforms to highlight the dips in the envelopes. Fig. 4(a), (b) and (c) shows the microwave waveforms after Gaussian windowing.

Fast Fourier transforms (FFTs) are then applied to the shaped microwave waveforms and three electrical spectra are acquired. To extract the envelopes from the microwave waveforms, the high frequency component of the microwave waveforms should be filtered out. A digital low-pass filter with a Gaussian function is implemented. Through properly adjusting the central frequency and the bandwidth of the low-pass filter, the high frequency component is filtered out. After filtering out the high frequency component, the microwave waveforms are recovered by performing an inverse fast Fourier transform (IFFT) to three filtered electrical spectra.

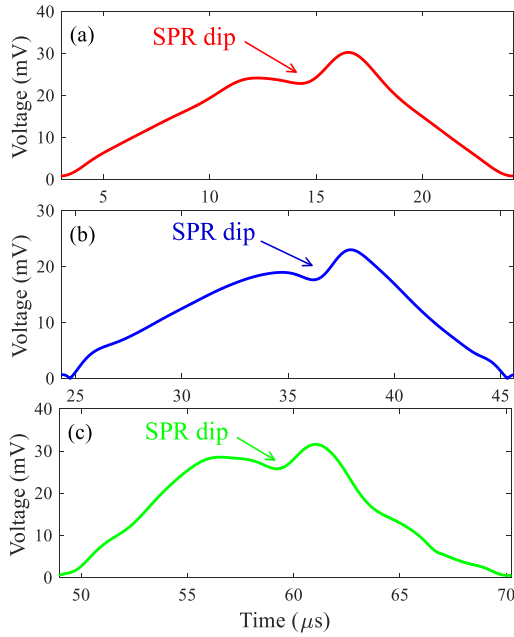


Fig. 5. The three envelopes extracted from the shaped waveforms resulted from (a) Au-TFBG1, (b) Au-TFBG2, and (c) Au-TFBG3.

Fig. 5(a), (b) and (c) shows the recovered microwave waveforms. As can be seen, the high frequency component of the three microwaves is filtered out and the envelopes are extracted. On the other hand, the recovered microwave waveforms agree well to the envelopes of the shaped microwave waveforms that shown in Fig. 4.

To evaluate the sensing performance of the proposed sensor, an experiment is performed. We immerse the Au-TFBG sensor array into a NaCl solution. By increasing the concentration of NaCl solution, the RI value of the NaCl solution is increased correspondingly and the changes of the envelopes extracted from the shaped microwave waveforms are monitored.

Fig. 6(a), (b) and (c) shows the changes of the extracted envelopes as the RI of the NaCl solutions is changed from 1.3325 to 1.3478. As can be seen that, when the RI of NaCl solutions increases, the dips in the extracted envelopes are shifted to a smaller time location. Then, the time shifts of the dip in the envelopes are measured and the sensing information is demodulated.

Fig. 7(a), (b) and (c) show the measured time shifts of the dip in the extracted envelopes as the RI of the NaCl solutions is changed from 1.3325 to 1.3478. As shown in the figures, the time locations of the dips are shifted from 13.59 to 11.72  $\mu\text{s}$ , 36.17 to 34.26  $\mu\text{s}$ , and 61.25 to 57.83  $\mu\text{s}$ . Considering the real-time oscilloscope has a sampling rate of 6.25 GS/s, the RI resolutions of the proposed sensor elements are calculated to be  $1.34 \times 10^{-6}$  RIU,  $1.25 \times 10^{-6}$  RIU and  $7.50 \times 10^{-7}$  RIU. These calculated RI resolutions are very high for the most of practical applications. Thus, the sampling rate can be reduced appropriately, and the parallel processing technique can be adopted to achieve an optimal sensing performance.

The stability of the proposed sensor is evaluated. In the experiment, the Au-TFBG array is immersed into a NaCl solution

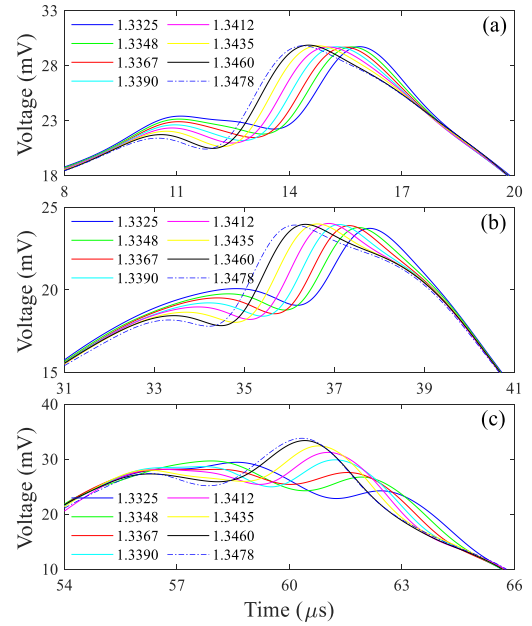


Fig. 6. The extracted envelopes when the ambient RI is changed from 1.3325 to 1.3478, (a) Au-TFBG1, (b) Au-TFBG2, and (c) Au-TFBG3.

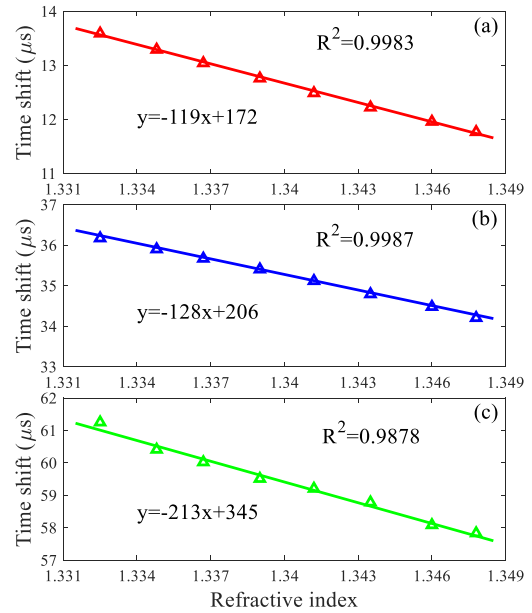


Fig. 7. The time shifts of the dips in the extracted envelopes as the ambient RI is changed from 1.3325 to 1.3478, (a) Au-TFBG1, (b) Au-TFBG2, and (c) Au-TFBG3.

with an RI value of 1.3325 within 15 minutes and the time shifts of the dips in the extracted envelopes are measured. The number of the time shift measurement is 200. Fig. 8(a), (b) and (c) show the measurement results. The maximum time shifts within 15 minutes of the three sensor elements are 10.3 ns, 9.2 ns and 15.2 ns. The sensing accuracy is also evaluated. The standard deviations of the three sensor elements are calculated to be 3.7 ns, 3.2 ns and 5.7 ns, corresponding to a measurement accuracy of  $3.1 \times 10^{-5}$  RIU,  $2.5 \times 10^{-5}$  RIU and  $2.6 \times 10^{-5}$  RIU. The accuracy measurements are poorer than those calculated

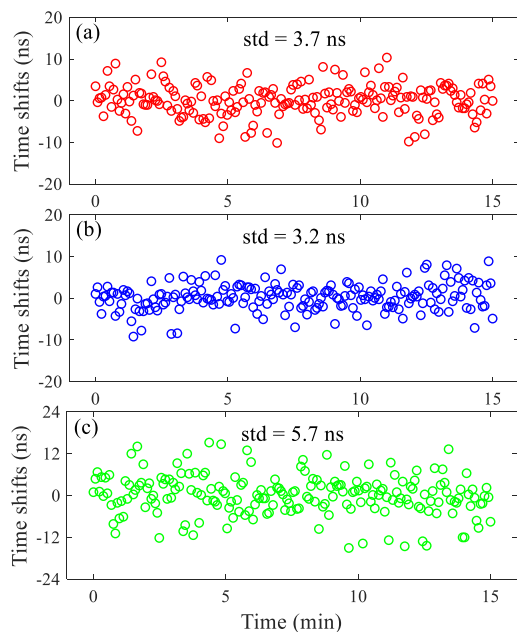


Fig. 8. The stability measurements of the sensor array with a measurement number of 200 within 15 minutes when the ambient RI is 1.3325, (a) Au-TFBG1, (b) Au-TFBG2, and (c) Au-TFBG3.

theoretically. The poorer sensing performance is mainly caused by the small drifting of the center wavelength of the TOF in the FDML laser source, which can be eliminated by performing a real-time calibration to the laser source.

#### IV. CONCLUSION

We proposed and experimentally demonstrated a high-speed and high-resolution multipoint RI sensing system based on an Au-TFBG sensor array using MWP interrogation method. The sensor array consists of three identical Au-TFBG sensors. Since the optical spectra of the Au-TFBGs are overlapped, the sensing information cannot be directly monitored in the optical domain. In the experiment, we converted the optical spectra of the Au-TFBG sensor array to the time domain based on SS-WTT mapping and separated the time domain signals with different time delays. A real-time oscilloscope was used to sample the temporal microwave waveforms in the time domain and a DSP was used to extract the envelopes at a high-speed and high-resolution. The sensing performance and stability of the proposed sensor were evaluated in the experiments by measuring the time shifts of the dip in the extracted envelopes. The accuracy measurements of the three sensor elements were  $3.1 \times 10^{-5}$  RIU,  $2.5 \times 10^{-5}$  RIU and  $2.6 \times 10^{-5}$  RIU and the sensing speed was as high as 11.75 kHz.

#### REFERENCES

- [1] M. Barozzi *et al.*, "Optical fiber sensors for label-free DNA detection," *J. Lightw. Technol.*, vol. 35, no. 16, pp. 3461–3472, Aug. 2017.
- [2] Y. Cao *et al.*, "Resolution-improved in situ DNA hybridization detection based on microwave photonic interrogation," *Opt. Exp.*, vol. 23, no. 21, pp. 27061–27070, Oct. 2015.
- [3] E. Fujiwara, L. E. da Silva, T. D. Cabral, H. E. de Freitas, Y. T. Wu, and C. M. de Barros Cordeiro, "Optical fiber specklegram chemical sensor based

- on a concatenated multimode fiber structure," *J. Lightw. Technol.*, vol. 37, no. 19, pp. 5041–5047, Oct. 2019.
- [4] X. He, Z. Ran, T. Yang, Y. Xiao, Y. Wang, and Y. Rao, "Temperature insensitive fiber-optic tip sensors array based on OCMR for multipoint refractive index measurement," *Opt. Exp.*, vol. 27, no. 7, pp. 9665–9675, Apr. 2019.
- [5] Y. Zhao *et al.*, "Torsion, refractive index, and temperature sensors based on an improved helical long period fiber grating," *J. Lightw. Technol.*, vol. 38, no. 8, pp. 2504–2510, Apr. 2020.
- [6] Z. Ding, T. Lang, Y. Wang, and C. Zhao, "Surface plasmon resonance refractive index sensor based on tapered coreless optical fiber structure," *J. Lightw. Technol.*, vol. 35, no. 21, pp. 4734–4739, Nov. 2017.
- [7] G. Wang *et al.*, "High-speed and high-resolution microwave photonic interrogation of a fiber-optic refractometer with plasmonic spectral comb," *J. Lightw. Technol.*, vol. 38, no. 7, pp. 2073–2080, Apr. 2020.
- [8] Z. Li, Y. Shen, Z. Yu, X. Ruan, Y. Zhang, and Y. Dai, "Polarization-dependent tuning property of graphene integrated tilted fiber Bragg grating for sensitivity optimization a numerical study," *J. Lightw. Technol.*, vol. 37, no. 9, pp. 2023–2035, May 2019.
- [9] X. Pham, J. Si, T. Chen, F. Qin, and X. Hou, "Wide range refractive index measurement based on off-axis tilted fiber Bragg gratings fabricated using femtosecond laser," *J. Lightw. Technol.*, vol. 37, no. 13, pp. 3027–3034, Jul. 2019.
- [10] Y. Liu, S. Li, H. Chen, J. Li, W. Zhang, and M. Wang, "Surface plasmon resonance induced high sensitivity temperature and refractive index sensor based on evanescent field enhanced photonic crystal fiber," *J. Lightw. Technol.*, vol. 38, no. 4, pp. 919–928, Feb. 2020.
- [11] R. Fan *et al.*, "Liquid level and refractive index double-parameter sensor based on tapered photonic crystal fiber," *J. Lightw. Technol.*, vol. 38, no. 14, pp. 3717–3722, Jul. 2020.
- [12] G. An, X. Hao, S. Li, X. Yan, and X. Zhang, "D-shaped photonic crystal fiber refractive index sensor based on surface plasmon resonance," *Appl. Opt.*, vol. 56, no. 24, pp. 6988–6992, Aug. 2017.
- [13] Y. Xiang *et al.*, "Quasi-distributed dual-parameter optical fiber sensor based on cascaded microfiber Fabry–Perot interferometers," *IEEE Photon. J.*, vol. 10, no. 2, pp. 1–9, Apr. 2018, Art. no. 2400309.
- [14] J. H. Lopez, O. Esteban, M. G. Shlyagin, and R. Martinez-Manuel, "Multipoint refractometer based on combined correlation and frequency multiplexing," *IEEE Photon. Technol. Lett.*, vol. 29, no. 17, pp. 1479–1482, Sep. 2017.
- [15] J. Yao, "Microwave photonics," *J. Lightw. Technol.*, vol. 27, no. 3, pp. 314–335, Feb. 2009.
- [16] J. Capmany and D. Novak, "Microwave photonics combines two worlds," *Nature Photon.*, vol. 1, pp. 319–330, Jun. 2007.
- [17] P. Ghelfi *et al.*, "A fully photonics-based coherent radar system," *Nature*, vol. 507, pp. 341–345, Mar. 2014.
- [18] R. A. Minasian, E. H. W. Chan, and X. Yi, "Microwave photonic signal processing," *Opt. Exp.*, vol. 21, no. 19, pp. 22918–22936, Sep. 2013.
- [19] S. Li *et al.*, "Optical vector analyzer with time-domain analysis capability," *Opt. Lett.*, vol. 46, no. 2, pp. 186–189, Jan. 2021.
- [20] T. Qing, S. Li, Z. Tang, B. Gao, and S. Pan, "Optical vector analysis with attometer resolution, 90-dB dynamic range and THz bandwidth," *Nature Commun.*, vol. 10, pp. 1–9, Nov. 2019.
- [21] J. Yao, "Photonic generation of microwave arbitrary waveforms," *Opt. Commun.*, vol. 284, no. 15, pp. 3723–3736, Jul. 2011.
- [22] R. Huber, M. Wojtkowski, and J. G. Fujimoto, "Fourier domain mode locking (FDML) a new laser operating regime and applications for optical coherence tomography," *Opt. Exp.*, vol. 14, no. 8, pp. 3225–3237, Apr. 2006.

**Guangying Wang** received the B.Eng. degree in optoelectronic information science and engineering from the Guangdong University of Technology, Guangzhou, China, in 2017. He is currently working toward the Ph.D. degree in optical engineering with the Institute of Photonics Technology, Jinan University, Guangzhou, China. His current research interests include microwave photonics sensing and signal processing.

**Baoliang Liao** received the B.Eng. degree in optoelectronic information science and engineering from Nanchang Hangkong University, Nanchang, China, in 2019. He is currently working toward the master's degree in optical engineering with the Institute of Photonics Technology, Jinan University, Guangzhou, China.

**Yuan Cao** received the B.S. degree from the Dalian University of Technology, Dalian, China, in 2011 and the Ph.D. degree from Jinan University, Guangzhou, China, in 2016. He is currently a Lecturer with the Institute of Photonics Technology, Jinan University. His research interests include microwave photonics signal processing & applications and optical biosensors.

**Tuan Guo** (M'07-SM'17) received the Ph.D. degree in optics from Nankai University, China, in 2007. From 2007 to 2010, he was a Postdoctoral Fellow with the Department of Electronics, Carleton University, Canada and the Photonics Research Centre, The Hong Kong Polytechnic University, respectively. Since 2010, he has been working with Jinan University, first as an Associate Professor and then as a Full Professor. Tuan Guo founded and currently heading the research activities of the Photonic Sensing for Energy & Biology Laboratory at the Institute of Photonics Technology (<https://ofscgroup.jnu.edu.cn/>). His current research interests include optical fiber sensors, plasmonics, biophotonics and photonics for renewable energy. He co-authored about 250 papers in peer-reviewed journals and international conferences, 2 book chapters and has been awarded over 20 patents from China and USA, respectively. He received the 2018 Technical Award of the IEEE Instrumentation and Measurement Society.

Dr. Guo is currently the IEEE-IMS technical committee chair of "Photonic Technology in Instrumentation and Measurement", a senior member of IEEE and a senior member of Optical Society of America. He is an Associate Editor for the IEEE/OSA JOURNAL OF LIGHTWAVE TECHNOLOGY, an Associate Editor for the SCIENCE CHINA Information Sciences. He has served as Associate TPC Chair for IEEE International Instrumentation and Measurement Technology Conference from 2019 to 2021, Session Chair of IEEE International Flexible Electronics Technology Conference 2018, TPC section Co-Chair of the CLEO Pacific Rim 2018.

**Xinhuan Feng** received the B.Sc. degree from Physics Department, Nankai University, Tianjin, China, in 1995, and the M.Sc. and Ph.D. degrees from the Institute of Modern Optics, Nankai University, in 1998 and 2005, respectively. From 2005 to 2008, she was a Postdoctoral Fellow with Photonics Research Centre, The Hong Kong Polytechnic University, Hong Kong. Since March 2009, she has been a Professor with the Institute of Photonics Technology, Jinan University, Guangzhou, China. Her research interests include various fiber active and passive devices and their applications, and microwave photonic signal processing.

**Bai-Ou Guan** (Member, IEEE, Fellow) received the B.Sc. degree in applied physics from Sichuan University, Chengdu, China, in 1994, and the M.Sc. and Ph.D. degrees in optics from Nankai University, Tianjin, China, in 1997 and 2000, respectively. From 2000 to 2005, he was with the Department of Electrical Engineering, The Hong Kong Polytechnic University, Hong Kong, first as a Research Associate, then as a Postdoctoral Research Fellow. From 2005 to 2009, he was with the School of Physics and Optoelectronic Engineering, Dalian University of Technology, Dalian, China, as a Full Professor. In 2009, he joined Jinan University, Guangzhou, China, where he founded the Institute of Photonics Technology. He has authored or coauthored more than 230 technical papers in peer-reviewed international journals and presented more than 30 invited talks at main international conferences. His current research interests include fiber optic devices and technologies, optical fiber sensors, biomedical photonic sensing and imaging, and microwave photonics. He was the recipient of the Distinguished Young Scientist Grant from Natural Science Foundation of China in 2012. He is a Member of OSA, and was a General Chair/Co-Chair, Technical Program Committee or Subcommittee Chair/Co-Chair for more than ten international conferences.

**Jianping Yao** (Fellow, IEEE) received the Ph.D. degree in electrical engineering from the Université de Toulon et du Var, France, in December 1997. He is currently a Distinguished University Professor and University Research Chair with the School of Electrical Engineering and Computer Science, University of Ottawa, Ottawa, ON, Canada. From 1998 to 2001, he was with the School of Electrical and Electronic Engineering, Nanyang Technological University, Singapore, as an Assistant Professor. In December 2001, he joined the School of Electrical Engineering and Computer Science, University of Ottawa, as an Assistant Professor, where he was promoted to an Associate Professor in May 2003, and a Full Professor in May 2006. He was appointed as an University Research Chair of microwave photonics in 2007. In June 2016, he was conferred the title of a Distinguished University Professor with the University of Ottawa. From July 2007 to June 2010 and from July 2013 to June 2016, he was the Director of the Ottawa-Carleton Institute for Electrical and Computer Engineering. He has authored or coauthored more than 620 research papers, including more than 360 papers in peer-reviewed journals and more than 260 papers in conference proceedings. Prof. Yao is the Editor-in-Chief of the IEEE PHOTONICS TECHNOLOGY LETTERS, a former Topical Editor of the *Optics Letters*, a former Associate Editor for the *Science Bulletin*, a Steering Committee Member of the IEEE JOURNAL OF LIGHTWAVE TECHNOLOGY, and an Advisory Editorial Board Member of the *Optics Communications*. He was a Guest Editor of the *Focus Issue on Microwave Photonics in Optics Express* in 2013, a Lead-Editor of the *Feature Issue on Microwave Photonics in Photonics Research* in 2014, and a Guest Editor of the special issue on microwave photonics in IEEE/OSA JOURNAL OF LIGHTWAVE TECHNOLOGY in 2018. Prof. Yao is currently the Technical Committee Chair of IEEE MTT-S Microwave Photonics and an Elected Member of the Board of Governors of the IEEE Photonics Society during 2019–2021. Prof. Yao was a Member of the European Research Council Consolidator Grant Panel in 2016, 2018, and 2020, the Qualitative Evaluation Panel in 2017, and a panelist of the National Science Foundation Career Awards Panel in 2016. Prof. Yao has also served as a Chair of a number of international conferences, symposia, and workshops, including the Vice Technical Program Committee (TPC) Chair of the 2007 IEEE Topical Meeting on Microwave Photonics, TPC Co-Chair of the 2009 and 2010 Asia-Pacific Microwave Photonics Conference, TPC Chair of the high-speed and broadband wireless technologies subcommittee of the IEEE Radio Wireless Symposium during 2009–2012, TPC Chair of the microwave photonics subcommittee of the IEEE Photonics Society Annual Meeting 2009, TPC Chair of the 2010 IEEE Topical Meeting on Microwave Photonics, General Co-Chair of the 2011 IEEE Topical Meeting on Microwave Photonics, TPC Co-Chair of the 2014 IEEE Topical Meetings on Microwave Photonics, General Co-Chair of the 2015 and 2017 IEEE Topical Meeting on Microwave Photonics, and General Chair of the 2019 IEEE Topical Meeting on Microwave Photonics. He also served as a committee member for a number of international conferences, such as IPC, OFC, CLEO, BGPP, and MWP. Prof. Yao was the recipient of the 2005 International Creative Research Award of the University of Ottawa. He was the recipient of the 2007 George S. Glinski Award for Excellence in Research. In 2008, he was awarded the Natural Sciences and Engineering Research Council of Canada Discovery Accelerator Supplements Award. Prof. Yao was selected to receive an inaugural OSA Outstanding Reviewer Award in 2012 and was one of the top ten reviewers of the IEEE/OSA JOURNAL OF LIGHTWAVE TECHNOLOGY 2015–2016. Prof. Yao was an IEEE MTT-S Distinguished Microwave Lecturer for 2013–2015. He was the recipient of the 2017–2018 Award for Excellence in Research of the University of Ottawa and was the recipient of the 2018 R.A. Fessenden Silver Medal from IEEE Canada. Prof. Yao is a registered Professional Engineer of Ontario. He is a Fellow of the Optical Society of America, the Canadian Academy of Engineering, and the Royal Society of Canada.